J. Biochem. 85, 21–28 (1979)

Physicochemical Properties of Pyocin F1

Kazufumi KURODA, Makoto KAGEYAMA,
Tadakazu MAEDA, and Satoru FUJIME

Mitsubishi-Kasei Institute of Life Sciences,
Minamiooya, Machida, Tokyo 194

Received for publication, June 17, 1978

The physicochemical properties of pyocin F1 were studied. Pyocin F1 consists of flexuous rod-like particles homogeneous in size. Each particle was composed of rod and fiber parts. The rod part was 105.5±9.5 nm long and 10.0±1.4 nm wide, and showed regular striations amounting to 23 layers. The fiber part was composed of several filaments; the length of the longest filament was 43.0±12.0 nm. The amino acid composition, the partial specific volume (0.720 ml/g), the sedimentation coefficient ($s^{0}_{20,w}$=35.1S), and the translational diffusion constant ($0.94 \pm 0.01 \times 10^{-7}$ cm^2/s) were determined. The particle weight was calculated to be 3.23×10^6 daltons.

In the preceding paper we showed that the flexuous rod-like particles produced by *Pseudomonas aeruginosa* P15 and P15-40 strains are a new bacteriocin (pyocin F1), distinct from pyocin R1 or phage PS10 which are both produced coincidentally by the same strains (*1*). These two bacteriocins and the phage were separated from each other and pyocin F1 was purified as a homogeneous protein from the mitomycin C-induced lysate of cells. The morphological resemblance of these bacteriocins to some bacteriophage tails may be significant. R-type pyocins with a contractile sheath are reminiscent of T-even coliphage tails, and pyocin F1 resembles the bacteriophage λ tail. Besides pyocin F1, several other flexuous bacteriocins, *i.e.*, bacteriocins resembling the bacteriophage λ tail, have been reported. Pyocin 28 (*2*, *3*) and pyocin 430f (*4*) are produced by *Pseudomonas aeruginosa*, various bacteriocins by some strains of *Serratia* (*5*), and bacteriocin 16-2 by a strain of *Rhizobium* (*6*). However, in comparison with R type pyocins, few biochemical studies of flexuous bacteriocins have been reported.

The present study describes the physicochemical properties of pyocin F1, including electron-microscopic structure, amino acid composition, sedimentation behavior, diffusion behavior, and molecular weight.

MATERIALS AND METHODS

Purification of Pyocin F1—*Pseudomonas aeruginosa* P15-40 was used as a pyocinogenic strain (*1*). The procedures of induction and purification were described previously (*1*). For amino acid analysis, analytical ultracentrifugation, and quasi-elastic light scattering, samples were further purified by sucrose density gradient centrifugation (*1*).

Electron Microscopy—All specimens were negatively stained as described previously (*1*) and examined under a JEOL 100B electron microscope at 80 kV. For determination of the dimensions of pyocin F1, images of pyocin F1 on electron micrographs in the magnification range from 105,000 to 356,000 times were traced using a quantitative picture-analyzing system, model MOP-01 (KONTRON). Pyocin R1 (129.0 nm) was used as an internal control (Y. Takeda, unpublished).

Amino Acid Analysis—Purified samples were sufficiently dialyzed against deionized water and then lyophilized. For acid hydrolysis, residues were treated with redistilled 6 N HCl containing 0.2% phenol at 110°C for 24 and 48 h. For the determination of sulfur-containing amino acids, samples were oxidized with performic acid according to the method of Moore (*7*) and hydrolyzed for 18 h. Hydrolyzed samples were analyzed using a Durrum type D-500 automatic amino acid analyzer. The Trp/Tyr ratio was estimated from the ultraviolet absorption curves of samples dissolved in 0.1 N NaOH and in 0.01 M Tris·Cl, 0.1 M NaCl, pH 7.5. Measurements were performed with a Cary type 17 recording spectrophotometer. The following values were used for the molar extinction coefficients in 0.1 N NaOH solution. Tyr at 294.4 nm, 2375; at 280 nm, 1576: Trp at 294.4 nm, 2375; at 280 nm, 5225.

Analytical Ultracentrifugation—Ultracentrifugation was performed in a Hitachi type 282 analytical ultracentrifuge at 20±0.6°C. Samples were dissolved in 0.01 M Tris and 0.1 M NaCl, pH 7.5. Runs were made at 5 protein concentrations, and measured with a UV system. Schlieren patterns were observed at the same time.

Quasi-Elastic Light Scattering—The translational diffusion coefficient of pyocin F1 particles was measured by the method of quasi-elastic light scattering. Pyocin F1 particles and light scattering cells were washed repeatedly with the above buffer after filtering it through 0.025 μm Millipore filters to remove dust particles. Pyocin F1 particles were finally suspended in dust-free buffer solution within the scattering cell. Concentrations of solutions were changed from 0.857 to 0.102 A_{280} unit.

The light source used was an argon laser of Coherent Radiation Co., model CR-4. The digital correlator used was the same as that reported previously (*8*) except that a NOVA minicomputer, instead of a multichannel pulse height analyzer, was used as an external memory. The sample cell was placed in a thermostatted oil bath. Measurements were carried out at scattering angles between 30° and 140° at intervals of 10° using 488 nm radiation.

The intensity autocorrelation functions, $g^{(2)}(\tau)$, of the light scattered from pyocin F1 solution were analyzed by the cumulant expansion method (*9*)

$$g^{(2)}(\tau)-1 \propto \exp[-\bar{\Gamma}\tau] \cdot \left(1+\frac{\mu_2}{2!}\tau^2-\frac{\mu_3}{3!}\tau^3+\cdots\right) \qquad (1)$$

to obtain the average decay constant ($\bar{\Gamma}$) divided by twice the square of the scattering vector (K^2), $\bar{\Gamma}/2K^2$, and the normalized dispersion, $\mu_2/\bar{\Gamma}^2$; at $K \rightarrow 0$ the former gives the z-averaged translational diffusion constant, D, and the latter is proportional to the width of the mol ecular weght distribution.

RESULTS

Structure of Pyocin F1—An electron micrograph of a purified pyocin F1 preparation is shown in Fig. 1a. Flexuous rod-like particles of homogeneous size are seen. One end of the rod appears to be square, but the other end tapers off to a point at which fiber-like structure (marked f) is observed. Fig. 1b shows the fine structure of pyocin F1. The fiber part appears to be composed of several long and short filaments, the number of which is not clear. Some globular structure is observed at the end of the longest filament, and at the junction of the filaments. A similar globular structure is occasionally found on the other short filaments. It is not known whether these globules are essential features of the pyocin F1 structure, or whether they are derived from cellular material, such as the receptor substance. Regular striations are present in the rod part. A dark central line is seen in some pyocin F1 rods (marked a in Fig. 1a), but the line is hardly visible in the distal region. Some particles have no such line (marked b). Figure 2 shows the length distributions of the rod and fiber parts of pyocin F1. The length of the pyocin F1 rod part seems to be uniform; for 85% of a total of 201 rods it was 105.5±9.5 nm (Fig. 2a). In the case of the fiber part, the longest filament was measured. As the filament is very thin and not well resolved, the observational error may be large. The distribution is shown in Fig. 2b; 88% of a total of 114 fibers gave a length of

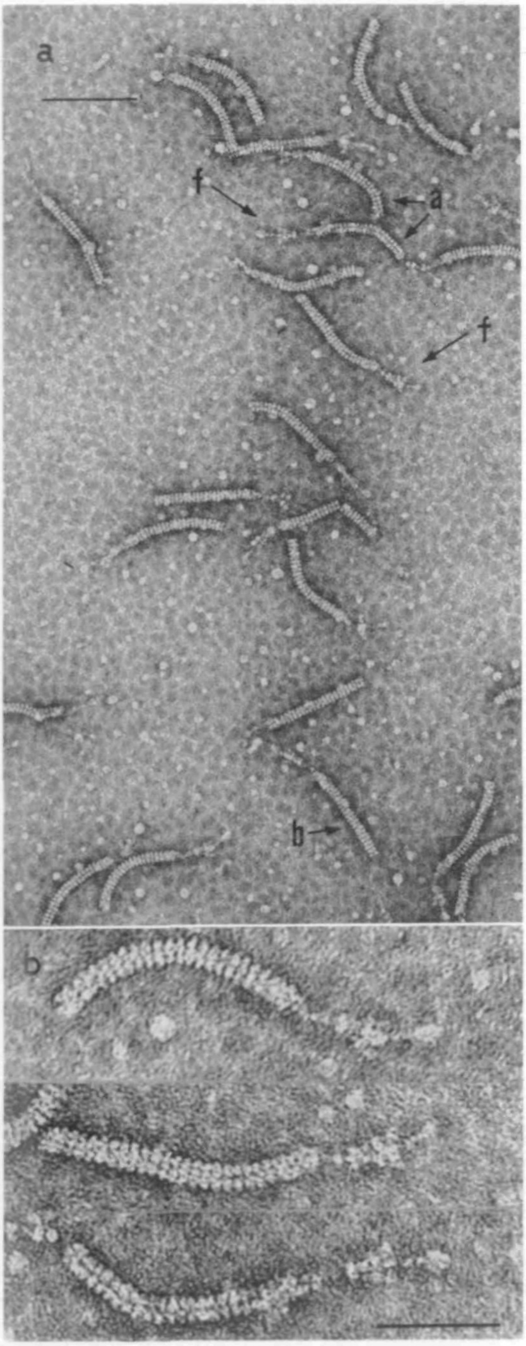

Fig. 1. Electron microscopy of purified pyocin F1. (a) The arrows show pyocin F1 particles with (a) and without (b) the dark central line, and the fiber part (f). The bar represents 100 nm. ×124,000. (b) Pyocin F1 particles at a higher magnification. The bar represents 50 nm. ×315,000.

43.0±12.0 nm. Therefore the total length is 149±12 nm. The width of pyocin F1 seems to be uniform, and 89% of a total ot 256 striations on 37 rods gave a value ot 10.0±1.4 nm (Fig. 3a). The number of striations was also counted. As a result of investigating 150 rods, the most frequent number of striations was found to be 23, excluding the distal part (Fig. 3b). Figure 4 summarizes these observations diagrammatically. The fiber part is shown tentatively as being composed of three filaments. The axial ratio of pyocin F1 was about 11 for the rod part and about 15 for the whole.

Amino Acid Analysis—The amino acid composition of pyocin F1 is shown in Table I, which gives the averages of two different preparations. The Trp/Tyr ratio, which was estimated spectrophotometrically as described in "MATERIALS AND METHODS," was found to be 1.96. Yui-Furihata pointed out a common feature in the

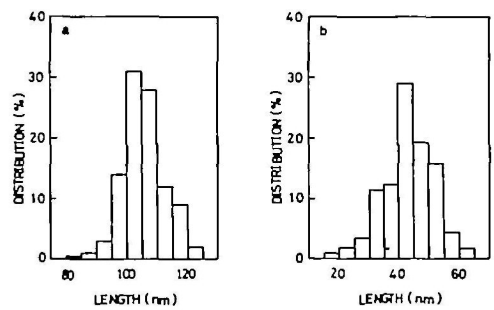

Fig. 2. Length distributions of the rod and fiber parts of pyocin F1. (a) The rod part, (b) the fiber part. Measurements were made on 201 rods and 114 fibers.

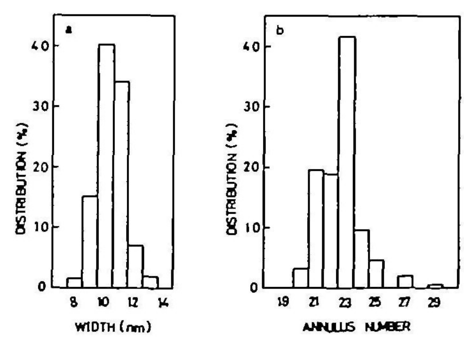

Fig. 3. Distributions of the width and the number of striations of pyocin F1. (a) The width, and (b) the striation number. Measurements were made on 256 rods for the width and 150 rods for the striations.

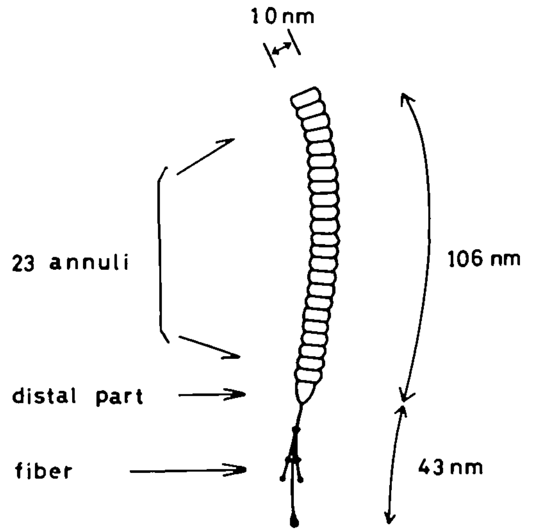

Fig. 4. Schematic representation of pyocin F1 structure.

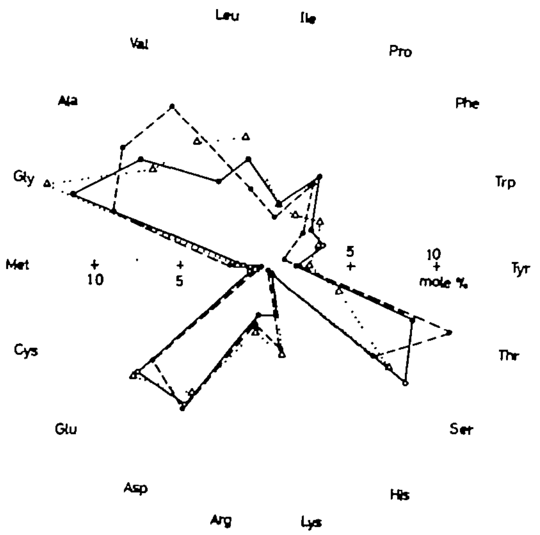

Fig. 5. Comparison of the amino acid compositions of pyocin F1, pyocin R1 core, and bacteriophage λ tail. —O—, Pyocin F1; ···△···, pyocin R1 core; --●--, bacteriphage λ tail.

amino acid composition of pyocin R1 and T-even coliphages, namely, high contents of Gly, Glu (+Gln), Asp (+Asn), Ser, Thr, and hydrophobic amino acids (*10*). The amino acid composition of pyocin F1 was similar in this respect (Fig. 5). The amino acid compositions of pyocin R1 core (*11*) and bacteriophage λ tail (*12*) are also shown in

TABLE I. Amino acid composition of pyocin F1.

Amino acid	Mol %
Asp	9.47
Thr	9.10[a]
Ser	10.66[a]
Glu	9.76
Pro	6.08
Gly	12.04
Ala	9.65
Cys	1.08[b]
Val	5.65
Met	1.38[b]
Ile	3.73
Leu	6.37
Tyr	1.73
Phe	3.30
His	0.61
Lys	2.98
Arg	3.04
Trp	3.39[c]
Sum	100.02

Values are expressed in mol percent and are averages of the values obtained with 24- and 48-h hydrolysates. [a] Values estimated by linear extrapolation to zero time of hydrolysis. [b] Values obtained with an 18-h hydrolysate of the performic acid-oxidized sample. [c] Estimated spectrophotometrically.

Fig. 5 for comparison. Though pyocin F1 and pyocin R1 core have a common feature, as described above, there are some differences in the amino acid compositions, *i.e.*, in the contents of Thr, Lys, Val, and Pro. In particular, the higher content of Pro of pyocin F1 and bacteriophage λ tail than pyocin R1 core is noteworthy. This provides further evidence that pyocin F1 is not a flexuous form of pyocin R1 core. The partial specific volume was calculated to be 0.720 ml/g using the values in Table I by the method of Cohn and Edsall (*13*).

Analytical Ultracentrifugation—Centrifugation was performed at 25,641 rpm with 5 serial dilutions (Fig. 6). At every concentration, the preparation showed a single sharp symmetrical peak. Figure 7 shows the most concentrated sample,

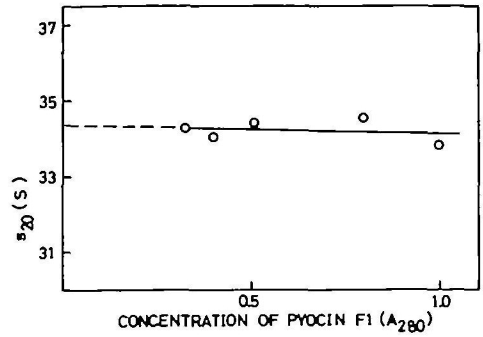

Fig. 6. Ultracentrifugal analysis of pyocin F1.

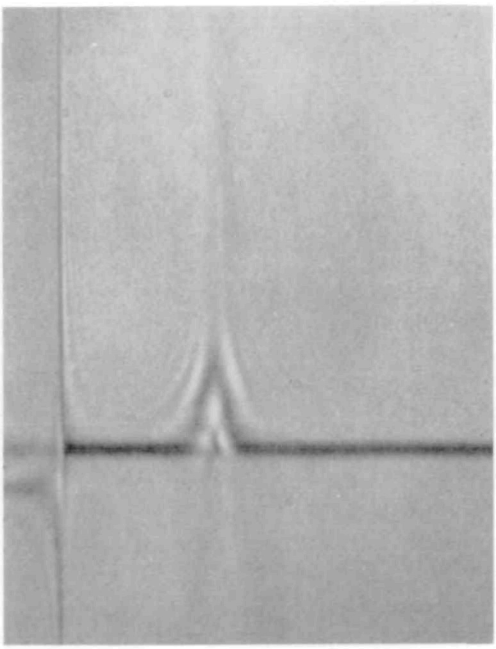

Fig. 7. Schlieren pattern of purified pyocin F1 in 0.01 M Tris-Cl–0.1 M NaCl, pH 7.5, 21 min after reaching 25,696 rpm at 20.0°C. A_{280}=1.00.

A_{280}=1.00. Extrapolating the s_{20} values to zero concentration, s^0_{20} was found to be 34.4S (Fig. 6). The $s^0_{20,w}$ value was calculated to be 35.1S, taking into account the concentration of NaCl and neglecting that of Tris in the buffer, and using the value of 0.720 (ml/g) for the partial specific volume.

Determination of the Diffusion Constant by Quasi-Elastic Light Scattering—The intensity autocorrelation functions of the light scattered from pyocin F1 solution at A_{280} values greater than 0.357 were well least-square-fitted by single

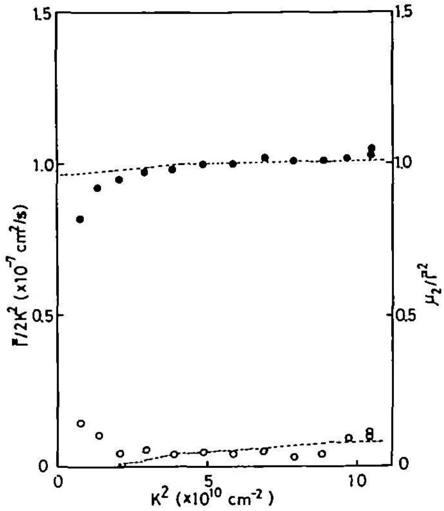

Fig. 8. An example of the relations among the average decay constant ($\bar{\Gamma}$) divided by twice the square of the scattering vector (K^2), $\bar{\Gamma}/2K^2$, the normalized dispersion, $\mu_2/\bar{\Gamma}^2$, and K^2, at 21.5°C in water (see the text). ●, ○, Observed values of $\bar{\Gamma}/2K^2$ and $\mu_2/\bar{\Gamma}^2$, respectively. ----, Theoretical curves for a rod with a length of 148 nm, including the effect of the rotational motion (see the text).

exponential decay curves at scattering angles higher than 60°, and gave almost constant values of $\bar{\Gamma}/2K^2$ and values of $\mu_2/\bar{\Gamma}^2$ smaller than 0.1 independent of the scattering angles (Fig. 8). At scattering angles lower than 50° or at the lowest concentration of the sample (0.102 A_{280} unit), they were no longer least-square-fitted by single exponential decay curves and gave smaller values of $\bar{\Gamma}/2K^2$ and larger values of $\mu_2/\bar{\Gamma}^2$. The departure of the correlation functions from single exponential decay curves can be interpreted as a result of contamination by dust particles larger than the pyocin F1 particles, *i.e.*, the lower the scattering angles, and the lower the concentration of pyocin F1, the greater the contribution of dust particles to the intensity of the scattered light. Thus we averaged the values of $\bar{\Gamma}/2K^2$ for samples with A_{280} greater than 0.357 at scattering angles higher than 60° and corrected for the effect of temperature to obtain $\bar{\Gamma}/2K^2=0.97\pm0.01\times10^{-7}$ cm²/s at 20°C in water. No concentration dependence of the value of $\bar{\Gamma}/2K^2$ was observed in the concentration range between 0.857 and 0.102 A_{280} unit (Fig. 9). The smaller value of $\bar{\Gamma}/2K^2$ at 0.102 A_{280} in Fig.

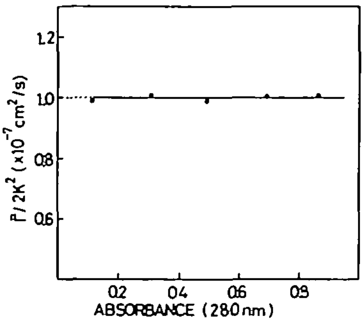

Fig. 9. The relation between the values of average decay constant divided by $2k^2$, $\bar{\Gamma}/2K^2$, and the concentration of pyocin F1 at 21.5°C.

9 does not represent concentration dependence, but contamination by dust particles as mentioned above.

At finite scattering angles, the value of $\bar{\Gamma}/2K^2$ is affected by the intramolecular Brownian motion of scattering molecules, such as rotation or flexing (*14*, *15*). Using a value of 149 nm for the length of pyocin F1, 3% of the above value of $\bar{\Gamma}/2K^2$ was attributable to the effect of rotational Brownian motion (*14*, *15*). Thus the translational diffusion constant, D_{tr}, at 20°C in water can be evaluated as $D_{tr}=0.94\pm0.01\times10^{-7}$ cm^2/s. The observed small values of $\mu_2/\bar{\Gamma}^2<0.1$ themselves and the results of computer simulation, including the effect of the rotational motion (----in Fig. 8), indicate that pyocin F1 particles are almost monodisperse, *i.e.*, homogeneous in size.

Particle Weight—The particle weight of pyocin F1 was calculated using Svedberg's equation, $M=R\cdot T\cdot s^0/(1-v^0\cdot\rho_0)\cdot D^\circ$, where M stands for particle weight, R is the gas constant (8.31×10^7 erg/deg.mol), T the absolute temperature (293.15 deg), ρ_0 the density of water at 20°C (0.9982 g/ml), and s°, V°, and D° are the sedimentation coefficient, partial specific volume, and diffusion constant in water at 20°C, respectively; the values used were 35.1×10^{-13} s, 0.720 ml/g, and 0.94×10^{-7} cm^2/s, respectively. From these data, the particle weight was calculated to be 3.23×10^6 daltons.

DISCUSSION

The present study shows that the pyocin F1 particle has a flexuous rod-like structure of uniform length, although some disrupted or anomalous structures are seen occasionally. The uniformity of our pyocin F1 preparation was confirmed not only by the patterns of sucrose density gradient centrifugation (*1*) and of analytical centrifugation (Fig. 7), but also by quasi-elastic light scattering measurements (Fig. 8). The structural characteristics of pyocin F1 are summarized in Fig. 4. Roughly speaking, it resembles the bacteriophage λ tail, but in detail, especially in the fiber parts, they are different (*16*, *17*).

As compared to other flexuous pyocins, F1 seems much more uniform than pyocin 28 reported by Takeya *et al.* (*2*, *3*). The length of pyocin 28 ranged from 20–400 nm, although rods of 100–120 nm were most frequent. The width was about 9 nm. In many rods, one end was square and the other end was sharp, sometimes having a fine fiber about 20 nm long. Pyocin 28 became attached to sensitive cells at this sharp end. A dark central line and cross-striations of 3.5 nm were usually observed. Therefore, pyocin 28 and pyocin F1 are similar as regards the striation pattern of the rod part, but differ in the length distribution and in the structure of the fiber part.

Govan gave no detailed description of the size and fine structure of his flexuous pyocin 430f (*4*).

Higerd *et al.* (*18*) observed a contractile pyocin produced by *P. aeruginosa* strain C_9(Ap$^-$). In their photographs, a flexible rod-like structure is often seen in addition to the contractile pyocin. They also found "highly-flexible polycores" exceeding 1 μm in length in their preparation. The striation patterns of these structures are again similar to those of pyocin F1 or pyocin 28. They suggested that these structures might be related to the core of the contractile pyocin (*18*).

As reported in the preceding paper (*1*), pyocin F1 was found in the lysate of strain P15, which also produced pyocin R1, a structure with a contractile sheath and a core. Hasegawa succeeded in separating the core from pyocin R1 and characterized it (*11*). We compared the core with F1 and found no relation between them. The results of subunit analysis, immunological reaction (*1*) and amino acid analysis (Table I) indicate that pyocin F1 is not a flexuous form of the pyocin R1 core.

Therefore, we presume that the flexuous "core" of Higerd *et al.* is unrelated to the core of R-type pyocin; it may be a different entity, possibly

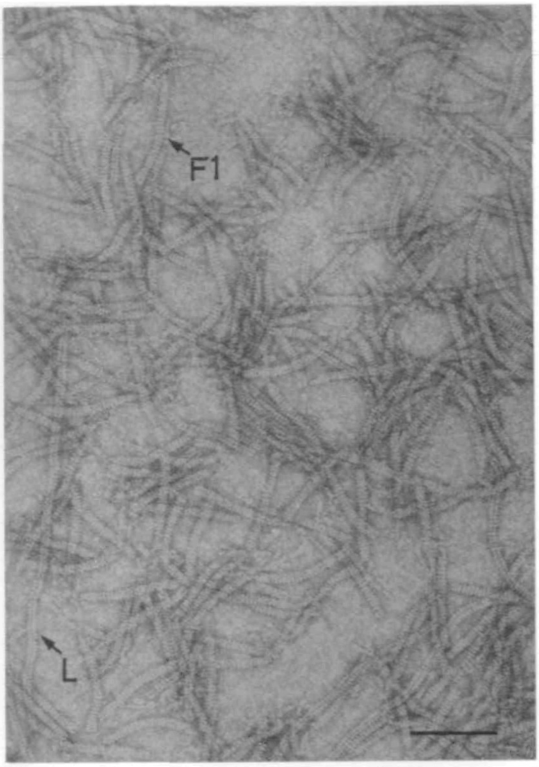

Fig. 10. Electron microscopy of a dense sample of purified pyocin F1 obtained by DEAE-cellulose chromatography. Besides pyocin F1 particles (F1) which are homogeneous in size, long tubes (L) are seen. The bar represents 100 nm. ×114,000.

another pyocin. We also found unusually long flexible rods in some samples of pyocin F1, which seem very similar to the "flexible polycores" of Higerd *et al.* (*18*), or to very long forms of pyocin 28 (*2*, *3*). This long structure was found in a concentrated fraction from DEAE-cellulose chromatography. As shown in Fig. 10, it is several times as long as the ordinary F1 particle, and the dark central line is observed all along the structure in every rod. The width of the rod and the interval of striation are the same as in pyocin F1. It is not clear whether one end tapers off to a point with fibers.

At this time we do not know whether this long structure is an aggregate of fragmented or intact pyocin F1, or a structure formed by mis-assembly during morphogenesis, or something else.

We determined the dimensions of pyocin F1 by calibrated electron microscopy. However, one can also estimate the particle length from its axial ratio and the experimental value of $\overline{\Gamma}/2K^2$ obtained by quasi-elastic light scattering measurements. The method is as follows. (i) Assume the particle is an ellipsoid of revolution having the axial ratio ρ. (ii) Assume $\overline{\Gamma}/2K^2$ is equal to the translational diffusion constant, D_{tr}, as the zeroth approximation. (iii) Calculate the length of the ellipsoid using the values of ρ and D by means of Perrin's equation (*19*, *20*). (iv) Estimate the contribution of the rotational diffusion of the particle to the value of $\overline{\Gamma}/2K^2$ (*14*, *15*) taking into account the effect of the finite channel width of the correlator (*8*), and correct the value of D assumed at step (ii). (v) Repeat steps (iii) and (iv) to obtain consistent results. Assuming the effective axial ratio of pyocin F1 to be 13 (see Fig. 4), the above procedure gave a value of 148 nm, which is in good agreement with the value, including the length of the fibers, obtained by electron microscopy.

No physical data, such as sedimentation coefficient and diffusion constant or molecular weight, have previously been reported for this kind of bacteriocin. Thus, pyocin F1 can now be used as a reference substance among bacteriocins.

We thank Miss M. Yokosawa for help in the preparation of purified pyocin F1, and Mr. S. Kondo for helpful advice regarding electron micrography.

REFERENCES

1. Kuroda, K. & Kageyama, M. (1979) *J. Biochem.* **85**, 7–19
2. Takeya, K., Minamishima, Y., Amako, K., & Ohnishi, Y. (1967) *Virology* **31**, 166–168
3. Takeya, K., Minamishima, Y., Ohnishi, Y., & Amako, K. (1969) *J. gen. Virol.* **4**, 145–149
4. Govan, J.R.W. (1974) *J. gen. Microbiol.* **80**, 17–30
5. Traub, W.H., Kleber, I., & Schaber, I. (1973) *Nature New Biology* **245**, 144–145
6. Gissmann, L. & Lotz, W. (1975) *J. gen. Virol.* **27**, 379–383
7. Moore, S. (1963) *J. Biol. Chem.* **238**, 235–237
8. Maeda, T. & Fujime, S. (1977) *J. Phys. Soc. Japan* **42**, 1983–1991
9. Koppel, D.E. (1972) *J. Chem. Phys.* **57**, 4814–4820
10. Yui-Furihata, C. (1972) *Tampakushitsu Kakusan Koso* (in Japanese) **17**, 165–175
11. Hasegawa, T. (1975) Ph.D. Thesis, Hokkaido University (in Japanese)

12. Buchwald, M., Steed-Claister, P., & Simmovitch, L. (1970) *Virology* **42**, 375–389
13. Schachman, H.K. (1957) in *Methods in Enzymology* (Colowick, S.P. & Kaplan, N.O., eds.) Vol. 4, pp. 32–103, Academic Press, New York
14. Pecora, R. (1964) *J. Chem. Phys.* **40**, 1604–1614
15. Cummins, H.Z., Carlson, F.D., Herbert, T.J., & Woods, G. (1969) *Biophys. J.* **69**, 518–546
16. Harrison, D.P., Brown, D.T., & Bode, V.C. (1973) *J. Mol. Biol.* **79**, 437–449
17. Mazza, A. & Felluga, B. (1973) *J. Ultrastruct. Res.* **45**, 259–278
18. Higerd, T.B., Baechler, C.A., & Berk, R.S. (1969) *J. Bacteriol.* **98**, 1378–1389
19. Perrin, F. (1934) *J. Phys. Radium* **5**, 497–511
20. Perrin, F. (1936) *J. Phys. Radium* **7**, 1–11